Development 139, 968-978 (2012) doi:10.1242/dev.065326

Regulation of cochlear convergent extension by the vertebrate planar cell polarity pathway is dependent on p120-catenin

Maria F. Chacon-Heszele[1,*], Dongdong Ren[1,2,*], Albert B. Reynolds[3], Fanglu Chi[2,‡] and Ping Chen[1,‡]

SUMMARY

The vertebrate planar cell polarity (PCP) pathway consists of conserved PCP and ciliary genes. During development, the PCP pathway regulates convergent extension (CE) and uniform orientation of sensory hair cells in the cochlea. It is not clear how these diverse morphogenetic processes are regulated by a common set of PCP genes. Here, we show that cellular contacts and geometry change drastically and that the dynamic expression of N-cadherin and E-cadherin demarcates sharp boundaries during cochlear extension. The conditional knockout of a component of the adherens junctions, p120-catenin, leads to the reduction of E-cadherin and N-cadherin and to characteristic cochlear CE defects but not misorientation of hair cells. The specific CE defects in p120-catenin mutants are in contrast to associated CE and hair cell misorientation defects observed in common PCP gene mutants. Moreover, the loss-of-function of a conserved PCP gene, *Vangl2*, alters the dynamic distribution of N-cadherin and E-cadherin in the cochlea and causes similar abnormalities in cellular morphology to those found in p120-catenin mutants. Conversely, we found that Pcdh15 interacts genetically with PCP genes to regulate the formation of polar hair bundles, but not CE defects in the cochlea. Together, these results indicate that the vertebrate PCP pathway regulates CE and hair cell polarity independently and that a p120-catenin-dependent mechanism regulates CE of the cochlea.

KEY WORDS: Adhesion, Cochlea, Planar cell polarity, Mouse

INTRODUCTION

The planar cell polarity (PCP) signaling pathway regulates a plethora of developmental and disease processes in vertebrates, including convergent extension (CE) of mesenchymal and neuroepithelial cells during gastrulation and neurulation (Keller, 2002; Keller and Tibbetts, 1989; Wallingford et al., 2000), and coordinated orientation of epithelial cells in the skin and the inner ear sensory organs (Curtin et al., 2003; Devenport and Fuchs, 2008; Guo et al., 2004; Montcouquiol et al., 2003). A common feature of these diverse processes is the polarization of neighboring cells along an axis parallel to the plane of the tissue (Vinson and Adler, 1987).

The PCP pathway consists of a set of conserved membrane and membrane-associated proteins known as core PCP proteins that regulate all the known PCP processes (Axelrod, 2009; McNeill, 2010; Strutt and Strutt, 2009). They include Flamingo (Usui et al., 1999), Van gogh (Vang) (Taylor et al., 1998) and Frizzled (Fz) (Vinson and Adler, 1987) receptors, and Dishevelled (Dsh) (Theisen et al., 1994). Numerous studies collectively show that these core PCP proteins orchestrate asymmetric membrane PCP protein complexes to guide the polarization of neighboring cells in a coordinated manner (Jones and Chen, 2007; Simons and Mlodzik, 2008). In vertebrates, ciliary genes are also required for PCP signaling, acting as a determinant of cell intrinsic polarity (Fischer and Pontoglio, 2009; Jones and Chen, 2008; Jones et al., 2008). Despite the shared feature of coordinated polarization of cells, epithelial PCP and CE in mesenchymal and epithelial tissues manifest in distinctive forms (Roszko et al., 2009; Simons and Mlodzik, 2008). Epithelial PCP is showcased by orienting a stable polar structure of the constituent cells coordinately among neighboring cells. CE in mesenchymal cells is characterized by polarized cellular protrusions along one planar axis. The polarized cellular protrusions exert concerted forces to drive the convergence of the cells along the same axis and result in concurrent extension of the tissue along a perpendicular axis (Keller, 2002; Wilson and Keller, 1991). In contrast to dynamic protrusive processes driving convergence of the mesenchymal cells towards the midline during gastrulation, the cohesion of the epithelium appears to be maintained in the neural plate during CE (Tada and Kai, 2009; Wang, J. et al., 2006). However, the morphological process for CE in the neuroepithelia has not been characterized.

The mechanisms by which divergent morphological polarization processes are regulated by common PCP genes are not well understood. In particular, several PCP processes may occur simultaneously in the same tissue, such as concurrent CE and establishment of epithelial PCP in the mammalian auditory organ during terminal differentiation. The mammalian hearing organ, the organ of Corti, contains a precisely patterned mosaic of sensory hair cells and non-sensory supporting cells along the length of the spiraled cochlear duct. Each hair cell in the cochlea is adorned with a V-shaped bundle of microvilli-derived stereocilia on its apical surface. In addition, a single primary cilium, known as the kinocilium, is asymmetrically positioned near the vertex of the V-shaped stereociliary bundle (Jones and Chen, 2008). All of the hair cells are oriented uniformly in the cochlea (Fig. 1). During terminal differentiation, hair cells and supporting cells of the organ of Corti

[1]Department of Cell Biology, Emory University, 615 Michael Street, Atlanta, Georgia 30322, USA. [2]Department of Otolaryngology, Eye, Ear, Nose and Throat Hospital, Fudan University, 220 Handan Road, Yangpu District, Shanghai 200433, China. [3]Department of Cancer Biology, Vanderbilt University, 211 Kirkland Hall, Nashville, TN 37240, USA.

*These authors contributed equally to this work
‡Authors for correspondence (chifanglu@yahoo.com.cn; ping.chen@emory.edu)

Accepted 21 December 2011

are both formed from a common pool of postmitotic cells packed in a shorter precursor domain that triples its length (Chen et al., 2002; McKenzie et al., 2004). Mutations in conserved PCP and ciliary genes cause both CE defects and misorientation or loss of polarity of hair cells (Jones and Chen, 2007; Jones and Chen, 2008; Wang et al., 2005). However, the morphogenetic processes of CE and hair cell alignment have not been characterized in depth, and it is not clear how these two concurrent but diverse PCP processes are executed under the regulation of a common set of core PCP and ciliary genes.

In this study, we characterized the cellular morphology of cochlear sensory epithelial cells during terminal differentiation and in mouse mutants that cause differential phenotypes in the two PCP processes. We provide evidence to support the hypothesis that the vertebrate PCP pathway regulates CE and epithelial PCP via distinct molecular modules in the cochlea.

MATERIALS AND METHODS

Mouse strains and animal care

Animal care and use was in accordance with US National Institutes of Health (NIH) guidelines and was approved by the Animal Care and Use Committee of Emory University. The following mouse strains were obtained from the Jackson Laboratories: Foxg1tm1(cre)Skm (*Foxg1^{Cre}*) with Cre knocked in at the *Foxg1* locus (Hebert and McConnell, 2000); Pcdh15(av-3j) (*Pcdh15^{3J}*) carrying a single nucleotide insertion that results in frameshift and a truncated protein lacking the transmembrane and cytoplasmic domains (Alagramam et al., 2001) and LPT/Le (*Vangl2^{Lp}*) carrying a single nucleotide G to A mutation, resulting in the change from serine to asparagine at the C terminal cytoplasmic domain (Kibar et al., 2001). The Polaris/IFT88-floxed strain (*Polaris$^{LoxP/LoxP}$*) was a gift from B. Yoder (University of Alabama, Birmingham, AL, USA) (Haycraft et al., 2007). The *p120$^{LoxP/LoxP}$* animals carry one LoxP site each in intron 2 and intron 8 at the *p120-catenin* locus (Davis and Reynolds, 2006). For staged embryos, the morning after mating was designated as embryonic day (E) 0.5.

Inner ear immunostaining and imaging

Standard procedures were used (Wang et al., 2005). The primary antibodies used in this study were raised against Arl13b (1:1500) (Caspary et al., 2007); Fzd3 (1:200) (Wang, Y. et al., 2006); γ-tubulin (Sigma, 1:200); p120-catenin (BD Laboratories, 1:200); E-cadherin (BD Laboratories, 1:200); N-cadherin (BD Laboratories, 1:400); and Sox2 (Santa Cruz, 1:200). Rhodamine- or Alexa Fluor 488-conjugated phalloidin (Invitrogen) were used for actin staining. Olympus SZX12 upright, Olympus FluoView FV-1000 confocal and Zeiss LSM510 confocal microscopes were used for image acquisition.

Analyses of stereociliary bundle orientation and morphology

The V-shaped hair bundle orientation was determined by drawing a line from the position of the kinocilium through the middle of the V-shaped stereocilia (bisecting line). We defined the angle of orientation as the angle formed between the bisecting line and the line parallel to the medial-to-lateral axis of the cochlear duct. Normally, this angle is close to 0°. Each row of hair cells was divided into three groups according to their position along the longitudinal axis of the cochlea (base, middle and apex) owing to the presence of a differentiation gradient within the cochlea during development. Only hair cells from the base and middle regions were included for quantification. At least 25 hair cells in each row in each region were quantified for each sample, and at least three animals per genotype were analyzed. The distribution of angles along the length of the cochlear duct was plotted using Oriana3 (Kovach Computing Services, Anglesey, Wales). Cells that had a central fonticulus were classified as having the maximum deviation, namely 180°. Mean data are presented. Statistical significance was analyzed by χ^2 analysis and Mardia Watson Wheeler tests using Oriana3.

Cellular morphogenesis analysis

For cellular morphogenesis and long axis quantification, we used Packing Analyzer software (http://idisk-srv1.mpi-cbg.de/~eaton/) (Aigouy et al., 2010) to extract the outline of cells from E14.5 cochlear samples stained with Phalloidin. Manual corrections of the outlines were done. The outlines were subjected to automated calculation of cellular long axis using a program we developed. The software is based on two computer vision development tools, Microsoft Visual C++ and Intel OpenCV Intel(R) Open Source Computer Vision Library. The long axis of the cells is designated as the Fit Line using the Least Squares method. The Fit Line is expressed in a linear regression function, $kx + b$. To determine the Fit Line, the following function,

$$D(k,b) = \sum_{i=1}^{N} (y_i - \mu(x_i))^2 = \sum_{i=1}^{N} (y_i - kx_i - b)^2, \quad (1)$$

was used to find the minimum of the sum of deviation,

$$\frac{\partial D}{\partial k} = -2\sum_{i=1}^{N} (y_i - b - kx_i)x_i = 0; \quad (2)$$

$$\frac{\partial D}{\partial b} = -2\sum_{i=1}^{N} (y_i - b - kx_i) = 0. \quad (3)$$

The slope (k) and intercept (b) of the Fit Line, $kx + b$, are determined by the following equations:

$$k = \frac{N\sum_{i=1}^{N} y_i x_i - \sum_{i=1}^{N} x_i \sum_{i=1}^{N} y_i}{N\sum_{i=1}^{N} x_i^2 - (\sum_{i=1}^{N} x_i)^2}; \quad (4)$$

$$b = \frac{\sum_{i=1}^{N} y_i \sum_{i=1}^{N} x_i^2 - \sum_{i=1}^{N} x_i \sum_{i=1}^{N} y_i x_i}{N\sum_{i=1}^{N} x_i^2 - (\sum_{i=1}^{N} x_i)^2}. \quad (5)$$

The angles between the Fit Line of each cell and the longitudinal axis of the cochlea duct were scored.

RESULTS

The developing organ of Corti undergoes drastic cellular morphogenesis during cochlear extension

The cells that give rise to the hair cells and supporting cells of the organ of Corti exit cell cycle between E12.5 and E14.5 in mice (Ruben, 1967). The newly postmitotic cells appear mostly as hexagonal cells at their apical surface with their long axes aligned with the longitudinal axis of the cochlear duct (Fig. 1A). By E18.5, the organ of Corti has differentiated and consists of one row of inner (IHC) and three rows of outer hair cells (OHC1-3) interdigitated with several types of non-sensory supporting cells, including inner phalangeal (Iph), inner (Ip) and outer pillar (Op), and Deiters' (DC1-3) cells (Fig. 1B). In contrast to the mostly uniform morphology in the undifferentiated organ of Corti, the cells in the differentiated organ of Corti have distinctive shapes with different cellular contacts at their apical surface. For example, the first and second rows of Deiters' cells have eight sides, whereas hair cells contact four neighboring cells (Fig. 1B). The maturation of the organ of Corti is accomplished by a graded differentiation process, which initiates near the base of the cochlea and progresses from the inner-most row to the outer-most row of hair cells and from the base to the apex of the cochlear duct (Fig. 1C-G). During this period, the length of the organ of Corti increases three- to fourfold, by a narrowing of the organ of Corti with no change in the number of cells (Chen et al., 2002). This type of tissue

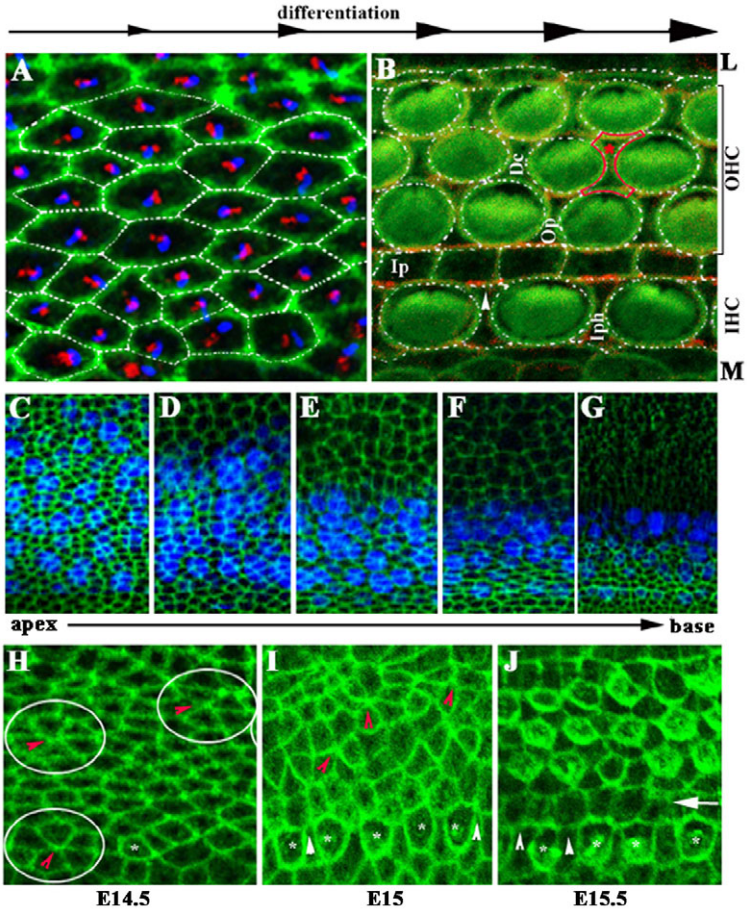

Fig. 1. Remarkable cellular contact remodeling and cell geometry changes during cochlear extension. (**A**,**B**) Surface views of the mouse cochlear epithelia at E14.5 (A) and postnatal day (P0) (B). The E14.5 cochlea (A) was stained for F-actin (green), γ-tubulin (red) and acetylated α-tubulin (blue), whereas the P0 cochlea (B) was stained for F-actin (green). IHC, inner hair cells; OHC, outer hair cells; Iph, inner phallangeal cells; Ip, inner pillar cells; Op, outer pillar cells; Dc, Deiters' cells; M and L, the center or medial side and the periphery or lateral side of the cochlear duct, respectively. Red lines and a red star outline a Dc (B). (**C-G**) Surface views of the cochlear duct at E14. Phalloidin (green) and Sox2 (blue) staining visualizes the outline of cells and the developing organ of Corti domain within the cochlear epithelium, respectively. (**H-J**) Surface views of the organ of Corti from E14.5 to E15.5. The samples were stained for F-actin. IHCs and the cellular rosettes are indicated by asterisks and circles, respectively. The distance between adjacent IHCs is indicated by white arrowheads. The white arrow marks the separation between IHCs and OHCs (J).

morphogenesis resembles CE in the establishment and extension of the body axes during gastrulation and in the extension and closure of the neural tube during neurulation (Keller, 2002).

Examination of cellular morphology revealed dynamic remodeling of cellular contacts during terminal differentiation. The vertices of the polygonal cells are exclusively tri-cellular prior to differentiation (Fig. 1A). As the organ of Corti differentiates, there are extensive cellular vertices formed by four cells (Fig. 1H,I) and by a rosette of five or more cells (Fig. 1H,I). The number of 4^{+}-cell vertices diminishes and gives way to again form tri-cellular vertices as the tissue elongates and the cells establish stable cellular contacts in a terminally differentiated organ (Fig. 1J). This process of cellular clustering and resolution implicates selective cellular contact shrinkage and extension during CE of the organ of Corti.

Dynamic expression of N-cadherin and E-cadherin demarcates sharp boundaries within the developing cochlea

A key component maintaining cell-cell contact or cell adhesion is cadherin-mediated adherens junctions (AJs). Classic experiments indicate that differential cell adhesion can drive tissue morphogenesis (Steinberg, 2007; Townes and Holtfreter, 1955), and recent studies show that cadherin-mediated AJs counter the contractile force generated by non-muscle myosin II and play a role in cellular morphogenesis during CE in *Drosophila* (Bertet et al., 2004; Rauzi et al., 2008; Zallen and Blankenship, 2008; Zallen and Wieschaus, 2004). To explore a potential role for AJs in cochlear CE, we examined the expression of E-cadherin (Cdh1 – Mouse Genome Informatics) and N-cadherin (Cdh2 – Mouse Genome Informatics) in the developing organ of Corti.

The earliest expression of E-cadherin appears at E15 and is readily detectable in cochlea at E15.5 (Fig. 2A-D). By E15, the nascent hair cells can be recognized by F-actin enrichment at their apical cortex (Fig. 2A-D). The expression level of E-cadherin continues to increase as the organ of Corti matures (Fig. 2A-H). Notably, the expression of E-cadherin is restricted to the OHC region and the region lateral to the outer hair cells, the Hensen cell region (Fig. 2A-H; supplementary material Fig. S1). In comparison to E-cadherin, N-cadherin had an earlier onset in the cochlea and could be detected at E14 (Fig. 2I,J). Complementary to the E-cadherin-expressing domain in the cochlea, the expression of N-cadherin is restricted to cells medial to the OHC region (Fig. 2I-N). A similar complementary expression of E-cadherin and N-cadherin in the cochlea at later stages has been reported previously (Etournay et al., 2010).

In summary, the expression of N-cadherin and E-cadherin is dynamic and defines a sharp boundary within the developing organ of Corti. The onset of E-cadherin membrane localization coincides with the stabilization of cell junctions in the region lateral to the inner pillar cells.

Inactivation of p120-catenin leads to reduction of cadherins and characteristic CE defects in the cochlea

The dynamic and precisely confined expression domains of N-cadherin and E-cadherin implicate a potential role for cadherins in demarcating specific cell populations within the cochlea and in mediating rapid cellular contact changes during CE of the cochlea. To explore their potential roles, we conditionally knocked out p120-catenin (Ctnnd1 – Mouse Genome

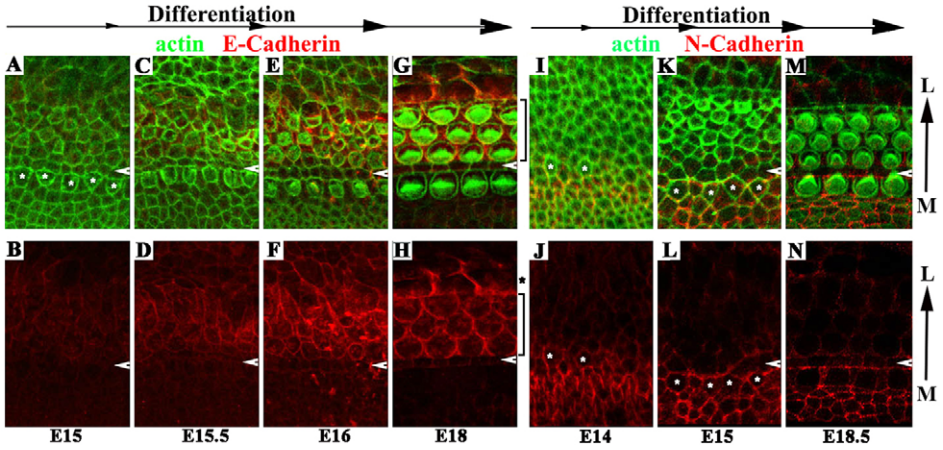

Fig. 2. Dynamic expression of N-cadherin and E-cadherin demarcates sharp boundaries within the developing organ of Corti. (**A-H**) Surface views of mouse cochleae from E15 to E18.5. The samples were stained for F-actin (green) and E-cadherin (red). The white arrowheads mark the separation between IHCs and OHCs. The OHC and Hensen cell regions are indicated by brackets and an asterisk, respectively (H). (**I-N**) Surface views of the organ of Corti from E14 to E18.5. The samples were stained for F-actin (green) and N-cadherin (red). The arrowheads and asterisks mark the separation between IHCs and OHCs, and the nascent IHCs, respectively. The medial (M) to lateral (L) arrows indicate the direction of PCP in the cochlea.

Informatics) in the inner ear (Davis and Reynolds, 2006). The p120-catenin protein binds to the intracellular domains of cadherins and stabilizes them at cell-cell junctions on cell membranes (Davis et al., 2003; Ireton et al., 2002; Xiao et al., 2007). Knockdown of p120-catenin leads to significant reduction of membrane cadherins in cultured cells and in vivo (Reynolds, 2007). We examined the expression of p120-catenin, and the effect of its loss on the levels of E-cadherin and N-cadherin in the cochlea (Fig. 3A-F; supplementary material Figs S1, S2). The p120-catenin protein was detected at cellular membranes in all of the epithelial cells in the control cochlea (Fig. 3A). We bred animals carrying the p120-catenin floxed allele with animals carrying a copy of Cre recombinase at the *Foxg1* locus (Hebert and McConnell, 2000) to inactivate *p120-catenin* in the cochlear epithelium. In $p120^{LoxP/LoxP}$; *Foxg1-Cre* ($p120^{CKO/CKO}$) cochleae, p120-catenin protein is barely detectable (Fig. 3B). As expected, the plasma membrane levels of E-cadherin are nearly abolished in $p120^{CKO/CKO}$ animals (Fig. 3C,D). The expression levels of N-cadherin are also greatly reduced in $p120^{CKO/CKO}$ cochleae (Fig. 3E,F). The reduction of cadherins in $p120^{CKO/CKO}$ animals was observed from the stage of their normal onset (supplementary material Figs S1, S2).

Despite the significant reduction of E-cadherin and N-cadherin in the cochlea, the general integrity of the organ of Corti is maintained in $p120^{CKO/CKO}$ animals at E18.5 (Fig. 3B,D,F,H). In addition, hair cells appear to have a normal polarity in the mutant animals (n=42) (Fig. 3G,H). We measured hair cell orientation from three control and three $p120^{CKO/CKO}$ mutant animals and confirmed that there was no statistically significant deviation of hair cell polarity in $p120^{CKO/CKO}$ animals (Fig. 3I-K). In the organ of Corti, several PCP proteins, such as Vangl2, have a polarized subcellular distribution parallel to the PCP axis (supplementary

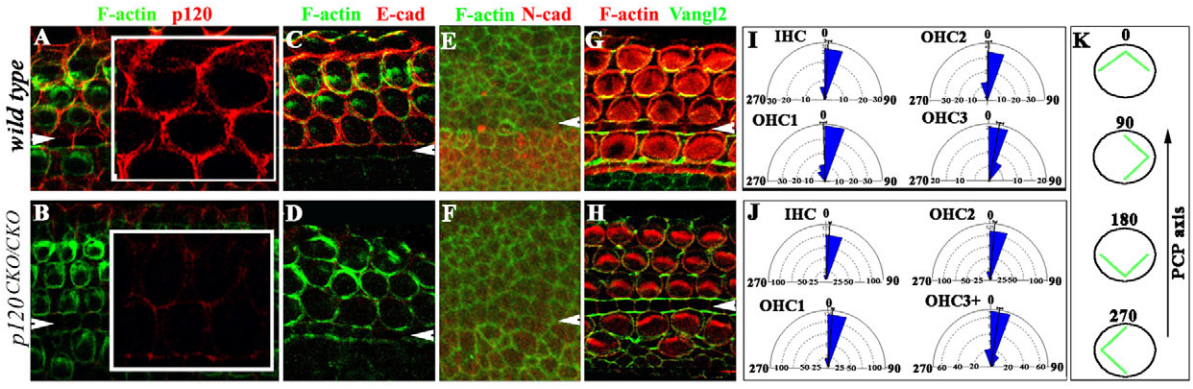

Fig. 3. Reduced levels of cadherins and normal hair cell polarity in $p120^{CKO/CKO}$ mice. (**A-F**) Surface views of the organs of Corti from E18.5 (A-D) and E14.5 (E,F) embryos. Wild-type (A,C,E) and $p120^{CKO/CKO}$ (B,D,F) samples were stained for F-actin (green) and p120-catenin (red) (A,B), F-actin (green) and E-cadherin (red) (C,D) or F-actin (green) and N-cadherin (red) (E,F). The boxes in A and B are the enlarged images of the organs of Corti from wild-type (A) and mutant (B) animals. The white arrowheads mark the inner pillar cell region that separates IHCs from OHCs. (**G**,**H**) Surface views of the organ of Corti from E18.5 wild-type (G) and $p120^{CKO/CKO}$ (H) animals carrying the *Vangl2-eGFP* transgene (green). F-actin (red) outlines the cellar cortex. (**I-K**) Oriana graphs showing the distribution of hair cell orientation from wild-type (I) and mutant (J) animals. The orientation of hair cells was determined (K) by measuring the angle formed between the medial-to-lateral axis of the cochlea and the line bisecting the stereociliary bundle from the center of the hair cell to the vertex of the hair bundle.

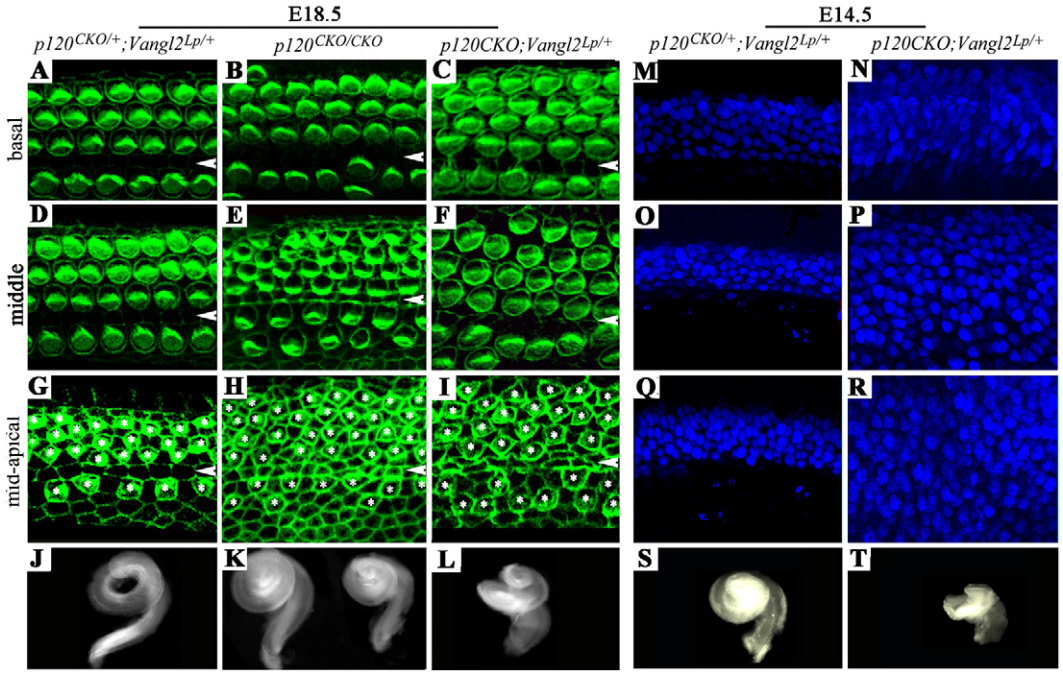

Fig. 4. *p120-catenin* conditional inactivation leads to the formation of a shorter and wider organ of Corti. (**A-T**) Cochleae from E18.5 (A-L) and E14.5 (M-T) control (A,D,G,J,M,O,Q,S), $p120^{CKO/CKO}$ (B,E,H,K) or $p120^{CKO/CKO};Vangl2^{Lp/+}$ (C,F,I,L,N,P,R,T) littermates were analyzed for their width by staining for F-actin (A-I, green) to visualize the rows of hair cells, and for their relative length (J-L,S,T) by measuring the total length of the cochlear ducts using ImageJ. Sox2 staining (M-R, blue) visualizes the width of the developing organ of Corti at E14.5. The arrowheads (A-I) and the asterisks (G-I) indicate the separation between IHCs and OHCs, and between the nascent neighboring IHCs, respectively.

material Fig. S3). In the organ of Corti from $p120^{CKO/CKO}$ animals, Vangl2 shows an asymmetric subcellular localization, similar to that of control animals (Fig. 3G,H).

There are, however, discernible patterning defects in the organ of Corti from $p120^{CKO/CKO}$ mutants at E18.5 (Fig. 3H, Fig. 4). Instead of the normal one row of inner and three rows of outer hair cells, additional rows of IHCs and OHCs are present (Fig. 3H, Fig. 4). This patterning defect was observed in 50% of the $p120^{CKO/CKO}$ mutants examined (n=30 animals). The cochlear duct is shortened in all of the $p120^{CKO/CKO}$ mutants that have a widened organ of Corti (Fig. 4A-L). The affected $p120^{CKO/CKO}$ cochleae have a length of 0.77±0.05 (n=3) relative to control littermates (1.00±0.02; n=3). The association of the widening and shortening of the cochlear duct has been observed in several PCP mutants, such as the looptail mutant with a loss-of-function mutation in *Vangl2* (Montcouquiol et al., 2003), the *Fz3* (*Fzd3* – Mouse Genome Informatics) and *Fz6* (*Fzd6* – Mouse Genome Informatics) (Fz3/6) double mutants (Wang, Y. et al., 2006), and the ciliary gene *Polaris* (*Ift88* – Mouse Genome Informatics) mutant (Jones et al., 2008). The association of these two phenotypes is considered to be indicative of CE defects. To test whether p120-catenin does indeed have a role in CE, we explored the genetic interaction between *p120-catenin* and *Vangl2*. *Vangl2* encodes a membrane protein with a C-terminal cytoplasmic tail. Point mutations at the C-terminal cytoplasmic region, the looptail mutations (Kibar et al., 2001), result in manifestation of all the known PCP defects. We crossed p120-catenin conditional knockout (CKO) with looptail animals. The $p120^{CKO/CKO};Vangl2^{Lp/+}$ animals generated (n=10) show 100% penetrance in cochlear shortening and widening (Fig. 4A-L). The severity of the CE defects in $p120^{CKO/CKO}$ and $p120^{CKO/CKO};Vangl2^{Lp/+}$ animals, however, is comparable.

The shortening and widening of the cochlear duct in p120-catenin mutants could be detected as early as E14.5 (Fig. 4M-T). We visualized the width of the organ of Corti prior to terminal differentiation by staining the developing cochlea with Sox2 to label the precursor cells of the organ of Corti at E14.5 (Fig. 4M-R) (Dabdoub et al., 2008). The precursor domain labeled by Sox2 at E14.5 is wider in $p120^{CKO/CKO};Vangl2^{Lp/+}$ samples along the length of the cochlear duct compared with heterozygous littermate $p120^{CKO/+}$, $Vangl2^{Lp/+}$ controls (Fig. 4M-R).

Together, the concomitant shortening and widening of the organ of Corti in the $p120^{CKO/CKO}$ or $p120^{CKO/CKO};Vangl2^{Lp/+}$ samples and the genetic interaction detected between p120-catenin and Vangl2 implicate a role for p120-catenin in regulating CE. Because cells undergo drastic morphological changes during CE to drive or accommodate exchanges of neighboring cells, we sought to determine whether there are cellular morphological defects associated with the patterning defects in affected $p120^{CKO/CKO}$ mutants (Fig. 5). We extracted cellular outlines (Aigouy et al., 2010) and developed a program to plot the long axis of each cell. This analysis identified morphological abnormalities in affected $p120^{CKO/CKO}$ cochleae (Fig. 5). In control animals, cells are mostly elongated along the longitudinal axis of the cochlear duct at E14.5 (Fig. 5A-E). In affected $p120^{CKO/CKO}$ littermates, there are more cells with their long axis not aligned with the longitudinal axis of the cochlear duct, especially towards the apex of the cochlea (Fig. 5F-J).

To explore further the potential morphological defects in $p120^{CKO/CKO}$ animals, we also quantified the percentage of vertices formed by three, and four or more cells in the control and $p120^{CKO/CKO}$ cochleae at E14.5 (Fig. 5K; supplementary material Table S1). As we described earlier (Fig. 1), there is an apparent cellular boundary shrinkage and resolution during cochlear extension. The tri-cellular vertices represent the pre-shrinkage or

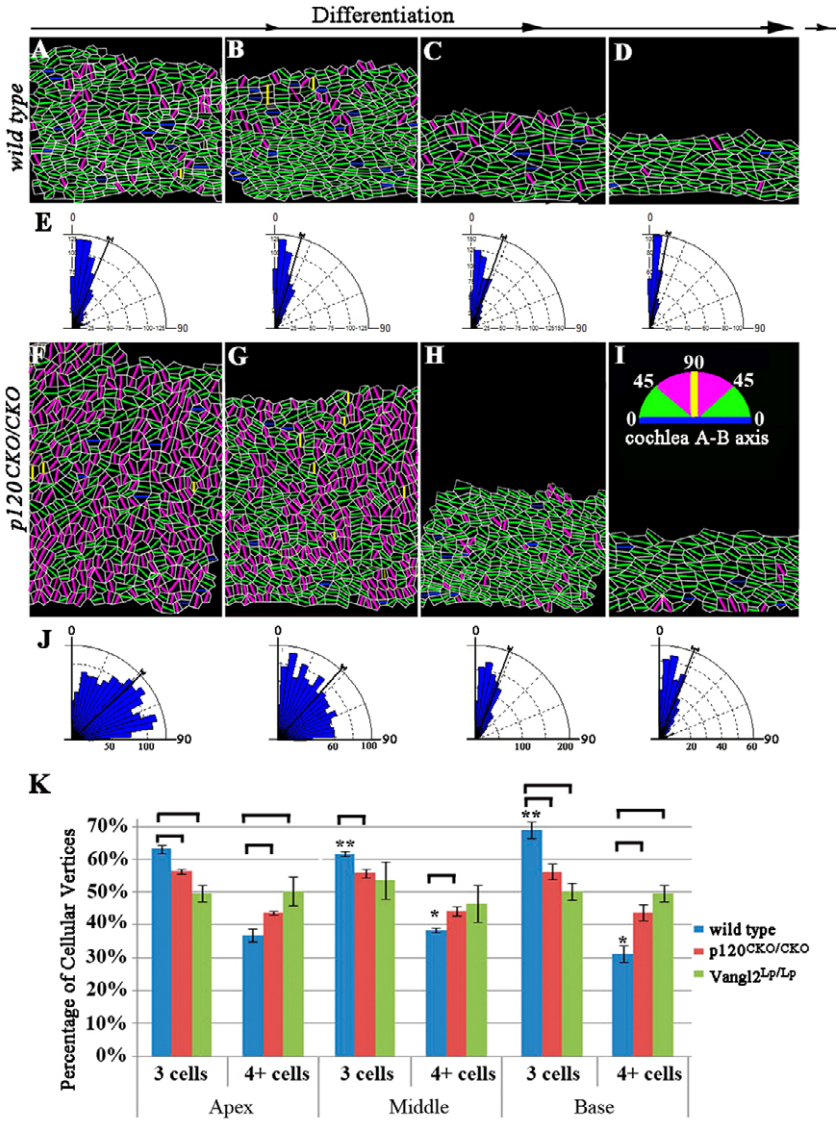

Fig. 5. The conditional inactivation of *p120-catenin* affects cellular morphology during CE. (**A-J**) The cellular outlines (A-D,F-I, white lines) in the developing organ of Corti in control (A-D) and $p120^{CKO/CKO}$ (F-I) E14.5 animals were extracted from F-actin-stained cochlear whole-mount images, and the cellular long axes were calculated and plotted. The distribution of the orientation of the long axis in the control (E) and $p120^{CKO/CKO}$ (J) is plotted using Oriana3 program. The colored lines indicate the angle that forms between the long axis of each cell and the longitudinal axis of the cochlear duct. (**K**) Quantification of tri-cellular and 4$^+$-cellular vertices. A total of ~3200 vertices were analyzed for each genotype. The percentage of cellular vertices formed by 3, 4 or 4$^+$ cells were counted in control (blue), $p120^{CKO/CKO}$ (red) and $Vangl2^{Lp/Lp}$ (green) animals at E14.5. The brackets and the matching asterisks indicate that the Welch's *t*-test *P*-value is less than 0.05 between the two conditions. Error bars represent s.d.

post-resolution states, whereas the vertices with four or more (4$^+$) cells are likely to correspond to a transitional state prior to resolution. There is a statistically significant difference in the number of transitional cellular vertices in the middle and the base of the cochlea (Fig. 5K; supplementary material Table S1). In the less differentiated middle region, there are more 4$^+$-cellular vertices than in the more differentiated basal region of the cochlea (Fig. 5K), suggesting that the less differentiated region has a large percentage of cells in transition. The comparison between control and $p120^{CKO/CKO}$ cochleae revealed a statistically significant difference (Fig. 5K; supplementary material Table S1). The $p120^{CKO/CKO}$ cochleae have more 4$^+$ or the transitional vertices than the controls (Fig. 5K). Similar results were observed for PCP mutant $Vangl2^{Lp/Lp}$ (Fig. 5K; supplementary material Table S1). The increased transitional state in $p120^{CKO/CKO}$ and $Vangl2^{Lp/Lp}$ cochleae implicates a similar defect in cellular resolution during CE.

Mutations in the PCP gene *Vangl2* alter the expression patterns of cadherins in the cochlea

It is conceivable that the requirement for p120-catenin for cochlear CE might be mediated by its role in modulating the levels of cadherins on the plasma membrane as there is an apparent defect in cellular resolution or in establishing new and stable cellular contacts. If so, it is possible that PCP signaling might regulate CE via cadherins.

We examined the expression of N- and E-cadherins in $Vangl2^{lp/lp}$ mutants that have defects in all the known PCP processes (Fig. 6). The sharp boundary defined by the expression of N-cadherin (Fig. 6A,B) is not present in the $Vangl2^{Lp/Lp}$ mice (Fig. 6C,D). The expression of N-cadherin in $Vangl2^{Lp/Lp}$ expands laterally past the normal boundary into the future OHC domain (Fig. 6C,D). The expression of E-cadherin is also altered in $Vangl2^{Lp/Lp}$ mutants (Fig. 6E-H). In $Vangl2^{Lp/Lp}$ mutants, the levels of E-cadherin at the cell membrane were drastically reduced (Fig. 6E-H). In addition, the relatively higher level of E-cadherin in the region lateral to the OHCs was not observed in $Vangl2^{Lp/Lp}$ littermates (Fig. 6E-H). Furthermore, we carried out western blot analysis and found that the levels of E-cadherin are significantly reduced in $Vangl2^{Lp/Lp}$ mutants (Fig. 6I,J).

Pcdh15 is required for hair cell polarity but is dispensable for cochlear extension

The requirement for p120-catenin in cochlear extension and the altered expression patterns of E-cadherin and N-cadherin in $Vangl2^{Lp/Lp}$ PCP mutants suggest that CE is mediated specifically

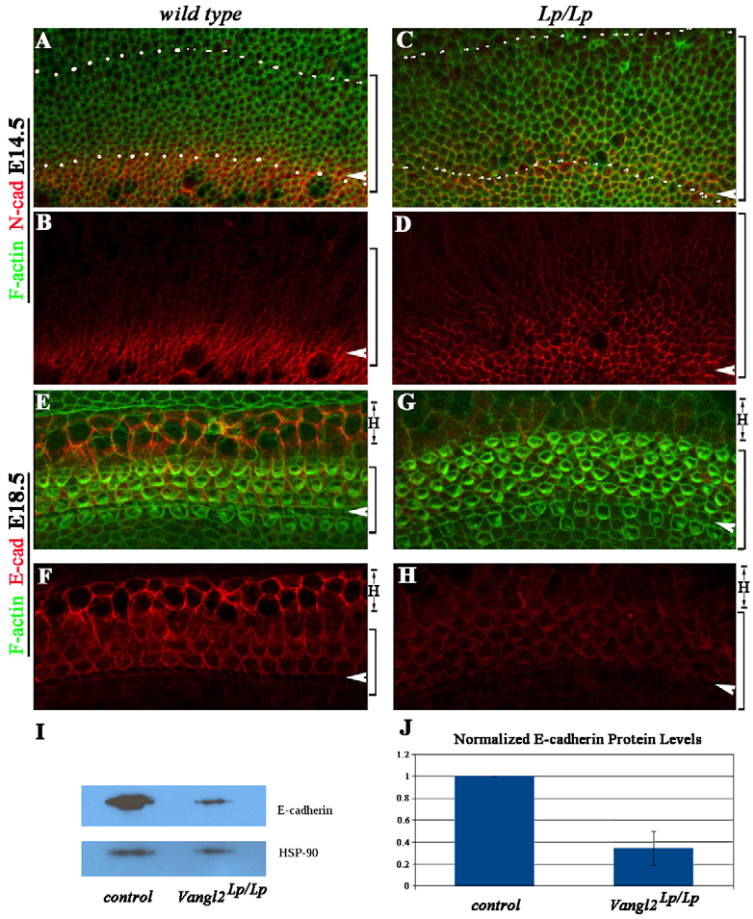

Fig. 6. Mutations in PCP gene *Vangl2* alter the expression of N-cadherin and E-cadherin in the cochlea. (**A-D**) Surface views of the cochleae from wild-type (A,B) and *Vangl2*$^{Lp/Lp}$ (C,D) animals at E14.5. Samples were stained for F-actin (green) and N-cadherin (red). Arrowheads mark the separation between IHCs and OHCs. The developing organ of Corti is identified by cellular morphology and cortical actin enrichment in the nascent hair cells, and is outlined between two dotted lines. (**E-H**) Surface views of the organs of Corti from wild-type (E,F) and *Vangl2*$^{Lp/Lp}$ (G,H) animals at E18.5. The samples were stained for F-actin (green) and E-cadherin (red). Arrowheads and 'H' mark the separation between IHCs and OHCs, and the Hensen cell region, respectively. (**I**,**J**) Western blot analysis (I) of E-cadherin proteins in the *Vangl2*$^{Lp/Lp}$ mutant and control cochleae, which is quantified and plotted (J). The densities of the Vangl2 protein bands were normalized with housekeeping proteins HSP-90 or α-tubulin (not shown) (J). Error bars represent s.d.

by a p120-catenin-dependent mechanism that probably involves E-cadherin and N-cadherin at the AJs. The specific requirement for p120-catenin in CE also implies that a molecular apparatus independent of p120-catenin regulates hair cell polarity in the cochlea. The polarity of hair cells is marked by the asymmetric positioning of the kinocilium and the basal body, and by the polar arrangement of stereocilia of graded heights. The machinery that builds the polar hair bundles is likely to interact with or be a part of the molecular module regulating hair bundle polarity. Components of the machinery for the formation of hair bundles were identified initially by their linkage to Usher syndrome, the most frequent hereditary cause of concomitant deafness and blindness in humans (El-Amraoui and Petit, 2005). A recent study further illustrates the detachment of the kinocilium from the stereocilia bundle and kinocilia mislocalization among Usher mutants (El-Amraoui and Petit, 2005; Lefevre et al., 2008). In particular, one of the Usher mutants, the *Pcdh15*$^{3J/3J}$ mutant, carrying a spontaneous loss-of-function mutation in *Protocadherin 15* (*Pcdh15*) (Alagramam et al., 2001), is one of the first Usher mutants with a reported mislocalization of the kinocilium (Ahmed et al., 2006; Ahmed et al., 2003; Senften et al., 2006).

To confirm a role for Pcdh15 in hair cell polarity, we analyzed the morphology of hair bundles and the position of the basal body in *Pcdh15*$^{3J/3J}$ mutants (supplementary material Fig. S4). The position of the kinocilium or the basal body can be readily identified by a structure known as the fonticulus, where the dense actin mesh formed elsewhere in the cuticular plate is absent. As reported previously, hair bundles in *Pcdh15*$^{3J/3J}$ mutants are disorganized and fragmented (supplementary material Fig. S4) (Alagramam et al., 2001; Lefevre et al., 2008). Compared with littermate controls, hair cells in *Pcdh15*$^{3J/3J}$ mutants have displaced and sometimes centrally positioned fonticulus (supplementary material Fig. S4A,B,K), confirming a defect in hair cell polarity. The normally polarized subcellular distribution of PCP protein Fz3, however, is maintained in *Pcdh15*$^{3J/3J}$ mutants (supplementary material Fig. S4C,D), similar to what was observed in a cilia mutant, *Polaris*$^{CKO/CKO}$ (Jones et al., 2008). Polaris is also known as intraflagellar protein 88 (Ift88) and is required for the formation of kinocilia (Jones et al., 2008). In *Polaris*$^{CKO/CKO}$ animals, both CE and hair cell polarity defects are present. Intriguingly, PCP proteins, including both Vangl2 and Fz3, show their normally polarized subcellular distribution despite the abnormality in hair bundle polarity in *Polaris*$^{CKO/CKO}$ animals (Jones et al., 2008), indicating that *Polaris* acts in parallel or downstream of the PCP genes *Vangl2* or *Fz3* in mediating hair cell polarity. In *Polaris*$^{CKO/CKO}$ animals, OHCs are misoriented and often lose their intrinsic polarity whereas the IHCs appear to maintain their normal hair bundle morphology and polarity (supplementary material Fig. S5) (Haycraft et al., 2007; Jones et al., 2008). The addition of a single *3J* allele of *Pcdh15* to *Polaris*$^{CKO/CKO}$ animals causes significant disruption to the polar arrangement of stereocilia in the IHCs (supplementary material Fig. S5).

In contrast to mutations of PCP genes that affect both hair cell polarity and CE of the cochlea, however, the loss-of-function of Pcdh15 specifically affects hair cell polarity but not extension of the cochlear duct (supplementary material Fig. S4E-K). *Pcdh15*$^{3J/3J}$ mutants showed a normal pattern of N-cadherin expression at

E14.5 and a normal cochlear length (supplementary material Fig. S4E-J). These observations together indicate that Pcdh15 is required only for hair cell polarity and interacts genetically with the ciliary and PCP gene polaris for the formation of the polar hair bundle.

DISCUSSION

The PCP pathway was characterized initially in *Drosophila* for its role in epithelial tissues (Simons and Mlodzik, 2008; Vinson and Adler, 1987). Studies in vertebrates showed that a set of conserved genes regulate additional cellular processes involving coordinated polarization of cells in multiple tissues (Keller, 2002; Mlodzik, 2002; Wallingford et al., 2000). However, the molecular modules that carry out morphological polarization for various forms of PCP remain obscure. It is not known whether different downstream effectors mediate the different manifestations of PCP forms. In this study, we presented evidence that the morphogenetic processes of CE and epithelial PCP are regulated by distinct molecular machineries downstream of common PCP genes.

Cellular morphogenesis during CE and other PCP processes

CE in vertebrates occurs in mesenchymal tissues during gastrulation and in the neural epithelium during neurulation (Keller, 2002). During gastrulation, the mesenchymal cells are polarized along one axis in the form of polarized and dynamic protrusive activities that create traction to pull the cells toward the midline and result in concomitant extension along a perpendicular axis: the future anterior-posterior axis. Cellular morphogenesis in epithelial tissues during CE is not well characterized in vertebrates. Studies in *Drosophila*, however, presented a lucid morphological description for epithelial CE. During *Drosophila* germband extension, cells in the gastrulating epiderm tissue transition from hexagonal cells to cellular rosettes by polar contraction of cellular contacts (Blankenship et al., 2006), or shrinkage of cellular contacts along one axis (Bertet et al., 2004). The formation of transient cellular rosettes is followed by polar expansion of cellular contacts along another axis perpendicular to the axis along which the initial shrinkage of cellular contacts occurs (Blankenship et al., 2006). Our characterization of cellular morphogenesis during cochlear extension in mice depicts a similar course. The organ of Corti is developed from a postmitotic domain consisting of tightly packed precursor cells that undergo rearrangements to achieve extension (Chen et al., 2002; McKenzie et al., 2004). We documented similar transitional phases of cellular rosettes and apparent resolution during cochlear extension (Figs 1, 5).

Other PCP processes include oriented cell divisions in multiple tissues, development of hair follicles in the dermis, and coordinated orientation of hair bundles in the inner ear sensory organs. The oriented cell division in epiblast cells during zebrafish axis elongation is accompanied by regulated cellular elongation (Gong et al., 2004). The development and orientation of hair follicles require regulated contraction and extension of cellular contacts within the same cell (Devenport and Fuchs, 2008). In the inner ear sensory organs, the formation of the polar hair bundle involves the relocation of the centrally positioned kinocilium to the periphery, formation of a dense F-actin mesh on the apical surface, the appearance of a V-shaped stereociliary bundle with graded heights, and the alignment of the pair of centrioles of the cell (Jones and Chen, 2008). Clearly, hair cell polarity manifests distinctively from CE process.

However, mutations in the conserved PCP genes, as well as a few general cytoskeleton regulators, cause multitudes of PCP defects. In the cochlea, the apparent CE defects are associated with hair bundle polarity in almost all of the known PCP mutants (Chacon-Heszele and Chen, 2009).

Distinct molecular regulation of epithelial CE and PCP in vertebrates

The underlying cellular and molecular mechanisms for the role of the vertebrate PCP pathway in regulating CE are not clear. In *Drosophila*, the contractile molecule Myosin 2 and adhesion molecule E-cadherin show planar polarization and complementary localization during germband extension and are required for the CE process, whereas the conserved PCP genes are not required (Bertet et al., 2004; Blankenship et al., 2006; Zallen and Wieschaus, 2004). In the mouse cochlea, we found that concomitant with apparent contraction and expansion of cellular contacts, the expression of the AJ proteins E-cadherin and N-cadherin at the cell membrane changes dynamically and marks a sharp boundary between the IHCs and OHCs of the cochlea (Fig. 2). Furthermore, the reduction of E-cadherin and N-cadherin levels at the plasma membrane through conditional inactivation of *p120-catenin* led to cellular morphological alterations (Fig. 5) and the formation of a shorter and wider cochlea (Fig. 4), suggesting a role for p120-catenin in regulation of selective cellular contacts and cellular morphogenesis during CE of the cochlea. Additional evidence supporting a role for p120-catenin in CE regulation during PCP signaling is the observed genetic interaction between p120-catenin and the conserved PCP gene *Vangl2*. In comparison to 50% penetrance of a CE defect in $p120^{CKO/CKO}$ animals (Fig. 4B,E,H,K), the addition of a single *Vangl2* loss-of-function allele resulted in complete penetrance of the phenotype (Fig. 4C,F,I,L).

These data support a role for p120-catenin in PCP signaling and implicate a direct involvement of E-cadherin and N-cadherin in mediating the requirement for p120-catenin in CE. The link between cell adhesion and tissue morphogenesis in vertebrates has been reported. Classic embryonic studies by Townes and Holtfreter (Townes and Holtfreter, 1955) and subsequent studies (Steinberg, 2007) show that differential adhesive properties of cells involving cadherins underlie cellular boundary formation, aggregation and, consequently, cellular movement. In particular, the notion that cell adhesion is linked to PCP morphogenesis processes and is directly regulated by the vertebrate PCP pathway has also emerged. E-cadherin is shown to play an essential role in zebrafish epiboly, a process in which the blastoderm and the yolk syncytial layer undergo radial intercalation to spread out and envelop the yolk (Kane et al., 2005; Shimizu et al., 2005). Non-canonical Wnt5 and Wnt11 can regulate the expression pattern of cadherins (Bradley and Drissi, 2011; Nagy et al., 2010); PCP signaling regulates cell adhesion properties of the zebrafish laterality organ (Oteiza et al., 2010); and PCP protein Vangl2 interacts with Rac1 to regulate AJs in the developing neural tube in mice (Lindqvist et al., 2010). Here, we showed that the levels of E-cadherin and N-cadherin are reduced significantly in $p120^{CKO/CKO}$ animals (Fig. 3). Moreover, the expression of E-cadherin and N-cadherin is abnormal in $Vangl2^{Lp/Lp}$ PCP mutant animals (Fig. 6). The levels of E-cadherin at the plasma membrane are reduced significantly in $Vangl2^{Lp/Lp}$ animals. The sharp border formed by the expression of N-cadherin within the organ of Corti is disrupted in $Vangl2^{Lp/Lp}$ animals (Fig. 6). Similar defects in resolution of cellular clusters are observed in both $p120^{CKO/CKO}$ and $Vangl2^{Lp/Lp}$ mutants. These data together support the suggestion that the regulation of cadherins by p120-catenin or

Vangl2 might underlie the common morphologic defect in resolving cellular clusters in the two mutants and the genetic interaction observed between the two genes (Figs 4, 5). Furthermore, together with the previous observation that interference of Myosin II function causes a CE defect in the cochlea (Yamamoto et al., 2009), our study supports a model that shares similarities with, but is also distinct from, CE regulation in *Drosophila*. Potentially, the counter action by Myosin II (Bertet et al., 2004; Zallen and Wieschaus, 2004) and adhesion molecules (Zallen and Wieschaus, 2004; Blankenship et al., 2006) plays similar roles in contraction and expansion of cellular contacts, respectively, to drive CE. Distinctively, this directional cellular contact remodeling is regulated by PCP signals in vertebrates, whereas unidentified signals independent of PCP genes in *Drosophila* control the polar distribution of E-cadherin and Myosin II during CE (Zallen and Wieschaus, 2004).

It is intriguing that the expression domains of N-cadherin and E-cadherin are sharply divided in the developing cochlea (Fig. 2). This raises the question of whether differential cadherin domains are essential for CE, given that cadherins have higher homophilic affinities and that differential adhesion is a fundamental driving force for tissue morphogenesis (Niessen et al., 2011; Townes and Holtfreter, 1955). The decreased level of E-cadherin in *Vangl2*$^{Lp/Lp}$ mutants probably reduces the differential adhesive force and contributes to the loss of N-cadherin expression boundary (Fig. 6). Furthermore, N-cadherin has an earlier onset whereas the expression of E-cadherin increases and correlates with the formation of mature cellular contacts (Fig. 2), indicating that the two cadherins might have differential roles in CE. Although both cadherins are type-I cadherins mediating cell adhesion, the expression of N-cadherin has been linked to cellular mobility whereas the expression of E-cadherin has an inverse correlation with increased mobility (Niessen et al., 2011). It is possible that, in addition to enforcing the segregation of two groups of hair cells during terminal differentiation, N-cadherin plays a major role at early steps of CE whereas E-cadherin aids the resolution of transient cellular clusters by establishing stable cellular contacts.

It is noted that the cochlea and vestibule have different requirement for p120-catenin for their integrity. The cochlear epithelium appears to maintain its integrity in p120-catenin mutants, despite the significant reduction of E-cadherin and N-cadherin (Figs 3, 4). β-Catenin binds to the cytoplasmic domain of cadherins and interacts with several proteins to build an adhesion complex and the cytoskeleton network. We found that β-catenin is localized to the plasma membrane in *p120*$^{CKO/CKO}$ animals (data not shown), implicating the presence of cadherins, such as remaining N- and E-cadherins and other cadherins, in *p120*$^{CKO/CKO}$ animals. Furthermore, members of Nectin proteins, also components of AJs, are present in the organ of Corti (Togashi et al., 2011). They probably retain their bridge with the cytoskeleton network to stabilize cell adhesion. It remains to be tested whether the cochlear epithelium in *p120*$^{CKO/CKO}$ animals can resist mechanical stress challenges. The utricle in the vestibule shows significant epithelial defects in *p120*$^{CKO/CKO}$ animals (supplementary material Fig. S6).

The cochleae from *p120*$^{CKO/CKO}$ showed normal hair cell polarity and normal localization of core PCP protein Fz3 (Fig. 3). The maintenance of polar distribution of core PCP proteins and hair cell polarity in *p120*$^{CKO/CKO}$ animals that are defective in CE implies independent regulations of CE and hair cell polarity by the vertebrate PCP pathway. Indeed, we confirmed a Pcdh15-dependent mechanism that is specific for regulating hair cell polarity. Mice homozygous for the functionally null *3J* mutation of *Pcdh15* (Alagramam et al., 2001) have no CE defects (supplementary material Figs S4, S5). However, hair cell polarization is disrupted in the *Pcdh15*$^{3J/3J}$ mice whereas the polar distribution of core PCP proteins is maintained (supplementary material Figs S4, S5), revealing a specific hair cell polarity defect downstream of core PCP genes in these mice. Furthermore, not only are many hair cells not properly aligned along the PCP axis, but in many instances they have a centrally located basal body/kinocilium, showing a loss of intrinsic cell polarization akin to that previously observed in ciliary mutants (Jones et al., 2008). The addition of a single copy of the loss-of-function mutant allele of *Pcdh15* in *Polaris*$^{CKO/CKO}$ animals gave rise to defects in stereociliary bundle morphology and polarity not found in *Polaris*$^{CKO/CKO}$ animals (supplementary material Figs S4, S5), suggesting a genetic interaction between polaris and *Pcdh15* in the formation of the polar stereociliary bundles. It is possible that the physical contribution of Pcdh15 to the linkers between the kinocilium and the nearby stereocilia underlies the genetic interaction between *Pcdh15* and the ciliary gene polaris.

Taken together, our study reveals distinct mechanisms downstream of core PCP genes in regulating CE and epithelial cell PCP. Cochlear CE is likely to be controlled via cadherin-dependent regulation of cell-cell contacts whereas the execution of hair cell planar cell polarity is regulated via a Pcdh15-dependent mechanism. The mechanism by which defects in core PCP signaling affect the regulation of cell-cell contacts is not known. The observations that N-cadherin and E-cadherin are abnormally distributed in core PCP mutants and that core PCP proteins colocalize with adhesion molecules (supplementary material Fig. S2) support the possibility that core PCP proteins directly regulate E-cadherin and N-cadherin to meet the requirement for cellular contact remodeling during CE. Similarly, how Pcdh15 or Pcdh15-containing complexes interpret polarity cues and interact with ciliary proteins to regulate the formation of the polar hair bundles has not been explored. Pcdh15 is a component of the physical links between the kinocilium and neighboring stereocilia and among stereocilia (Ahmed et al., 2006; Kazmierczak et al., 2007; Muller, 2008), and its isoforms have been localized to the basal body area (Ahmed et al., 2003; Alagramam et al., 2007; Senften et al., 2006). It is possible that the physical links between the kinocilium and adjacent stereocilia are essential for the proper transmission of the polarity cues from polarized core PCP complexes to the polar localization of the kinocilium, which is essential for the intrinsic polarity of hair cells (Jones et al., 2008). Alternatively, Pcdh15 or Pcdh15-containing complexes could directly control the polarization of the kinocilium downstream of core PCP protein complexes, leading to subsequent cohesive patterning and orientation of the stereociliary bundle. Nonetheless, the regulation of CE and hair cell polarity via p120-catenin- and Pcdh15-mediated mechanisms by the PCP pathway probably both involve actin and microtubule cytoskeleton components that form distinct and perhaps compartmented complexes for cellular morphogenesis and for polar positioning of the kinocilium.

Acknowledgements

We thank Drs B. Yoder, T. Caspary, J. Nathans, S. Li and M. Kelly for reagents and comments and Dr D. Eaton, Mr E. Eaton and the Department of Physiology at Emory University for the use of the Olympus FluoView FV-1000 confocal microscope.

Funding

This study was supported by National Institutes of Health grants [RO1 DC007423 and DC005213 to P.C.]; Natural Science Foundation of China (NSFC) grants [81028003/H1305 to P.C. and F.C., and 81000413/H1305 to D.R.]; Shanghai Rising-Star Program A-type grant [11QA1401100] and the Research Fund for the Doctoral Program of High Education grant

[20110071120086] to D.R.; and was supported in part by the Neuronal Imaging Core of the Emory Neuroscience National Institute of Neurological Disorders and Stroke (NINDS) Core Facilities grant [P30NS055077]. Deposited in PMC for release after 12 months.

Competing interests statement

The authors declare no competing financial interests.

Supplementary material

Supplementary material available online at
http://dev.biologists.org/lookup/suppl/doi:10.1242/dev.065326/-/DC1

References

Ahmed, Z. M., Riazuddin, S., Ahmad, J., Bernstein, S. L., Guo, Y., Sabar, M. F., Sieving, P., Griffith, A. J., Friedman, T. B., Belyantseva, I. A. et al. (2003). PCDH15 is expressed in the neurosensory epithelium of the eye and ear and mutant alleles are responsible for both USH1F and DFNB23. *Hum. Mol. Genet.* **12**, 3215-3223.

Ahmed, Z. M., Goodyear, R., Riazuddin, S., Lagziel, A., Legan, P. K., Behra, M., Burgess, S. M., Lilley, K. S., Wilcox, E. R., Griffith, A. J. et al. (2006). The tip-link antigen, a protein associated with the transduction complex of sensory hair cells, is protocadherin-15. *J. Neurosci.* **26**, 7022-7034.

Aigouy, B., Farhadifar, R., Staple, D. B., Sagner, A., Roper, J. C., Julicher, F. and Eaton, S. (2010). Cell flow reorients the axis of planar polarity in the wing epithelium of *Drosophila*. *Cell* **142**, 773-786.

Alagramam, K. N., Murcia, C. L., Kwon, H. Y., Pawlowski, K. S., Wright, C. G. and Woychik, R. P. (2001). The mouse Ames waltzer hearing-loss mutant is caused by mutation of Pcdh15, a novel protocadherin gene. *Nat. Genet.* **27**, 99-102.

Alagramam, K. N., Miller, N. D., Adappa, N. D., Pitts, D. R., Heaphy, J. C., Yuan, H. and Smith, R. J. (2007). Promoter, alternative splice forms, and genomic structure of protocadherin 15. *Genomics* **90**, 482-492.

Axelrod, J. D. (2009). Progress and challenges in understanding planar cell polarity signaling. *Semin. Cell Dev. Biol.* **20**, 964-971.

Bertet, C., Sulak, L. and Lecuit, T. (2004). Myosin-dependent junction remodelling controls planar cell intercalation and axis elongation. *Nature* **429**, 667-671.

Blankenship, J. T., Backovic, S. T., Sanny, J. S., Weitz, O. and Zallen, J. A. (2006). Multicellular rosette formation links planar cell polarity to tissue morphogenesis. *Dev. Cell* **11**, 459-470.

Bradley, E. W. and Drissi, M. H. (2011). Wnt5b regulates mesenchymal cell aggregation and chondrocyte differentiation through the planar cell polarity pathway. *J. Cell. Physiol.* **226**, 1683-1693.

Caspary, T., Larkins, C. E. and Anderson, K. V. (2007). The graded response to Sonic Hedgehog depends on cilia architecture. *Dev. Cell* **12**, 767-778.

Chacon-Heszele, M. F. and Chen, P. (2009). Mouse models for dissecting vertebrate planar cell polarity signaling in the inner ear. *Brain Res.* **1277**, 130-140.

Chen, P., Johnson, J. E., Zoghbi, H. Y. and Segil, N. (2002). The role of Math1 in inner ear development: Uncoupling the establishment of the sensory primordium from hair cell fate determination. *Development* **129**, 2495-2505.

Curtin, J. A., Quint, E., Tsipouri, V., Arkell, R. M., Cattanach, B., Copp, A. J., Henderson, D. J., Spurr, N., Stanier, P., Fisher, E. M. et al. (2003). Mutation of Celsr1 disrupts planar polarity of inner ear hair cells and causes severe neural tube defects in the mouse. *Curr. Biol.* **13**, 1129-1133.

Dabdoub, A., Puligilla, C., Jones, J. M., Fritzsch, B., Cheah, K. S., Pevny, L. H. and Kelley, M. W. (2008). Sox2 signaling in prosensory domain specification and subsequent hair cell differentiation in the developing cochlea. *Proc. Natl. Acad. Sci. USA* **105**, 18396-18401.

Davis, M. A. and Reynolds, A. B. (2006). Blocked acinar development, E-cadherin reduction, and intraepithelial neoplasia upon ablation of p120-catenin in the mouse salivary gland. *Dev. Cell* **10**, 21-31.

Davis, M. A., Ireton, R. C. and Reynolds, A. B. (2003). A core function for p120-catenin in cadherin turnover. *J. Cell Biol.* **163**, 525-534.

Devenport, D. and Fuchs, E. (2008). Planar polarization in embryonic epidermis orchestrates global asymmetric morphogenesis of hair follicles. *Nat. Cell Biol.* **10**, 1257-1268.

El-Amraoui, A. and Petit, C. (2005). Usher I syndrome: unravelling the mechanisms that underlie the cohesion of the growing hair bundle in inner ear sensory cells. *J. Cell Sci.* **118**, 4593-4603.

Etournay, R., Lepelletier, L., Boutet de Monvel, J., Michel, V., Cayet, N., Leibovici, M., Weil, D., Foucher, I., Hardelin, J. P. and Petit, C. (2010). Cochlear outer hair cells undergo an apical circumference remodeling constrained by the hair bundle shape. *Development* **137**, 1373-1383.

Fischer, E. and Pontoglio, M. (2009). Planar cell polarity and cilia. *Semin. Cell Dev. Biol.* **20**, 998-1005.

Gong, Y., Mo, C. and Fraser, S. E. (2004). Planar cell polarity signalling controls cell division orientation during zebrafish gastrulation. *Nature* **430**, 689-693.

Guo, N., Hawkins, C. and Nathans, J. (2004). Frizzled6 controls hair patterning in mice. *Proc. Natl. Acad. Sci. USA* **101**, 9277-9281.

Haycraft, C. J., Zhang, Q., Song, B., Jackson, W. S., Detloff, P. J., Serra, R. and Yoder, B. K. (2007). Intraflagellar transport is essential for endochondral bone formation. *Development* **134**, 307-316.

Hebert, J. M. and McConnell, S. K. (2000). Targeting of cre to the Foxg1 (BF-1) locus mediates loxP recombination in the telencephalon and other developing head structures. *Dev. Biol.* **222**, 296-306.

Ireton, R. C., Davis, M. A., van Hengel, J., Mariner, D. J., Barnes, K., Thoreson, M. A., Anastasiadis, P. Z., Matrisian, L., Bundy, L. M., Sealy, L. et al. (2002). A novel role for p120 catenin in E-cadherin function. *J. Cell Biol.* **159**, 465-476.

Jones, C. and Chen, P. (2007). Planar cell polarity signaling in vertebrates. *BioEssays* **29**, 120-132.

Jones, C. and Chen, P. (2008). Primary cilia in planar cell polarity regulation of the inner ear. *Curr. Top. Dev. Biol.* **85**, 197-224.

Jones, C., Roper, V. C., Foucher, I., Qian, D., Banizs, B., Petit, C., Yoder, B. K. and Chen, P. (2008). Ciliary proteins link basal body polarization to planar cell polarity regulation. *Nat. Genet.* **40**, 69-77.

Kane, D. A., McFarland, K. N. and Warga, R. M. (2005). Mutations in half baked/E-cadherin block cell behaviors that are necessary for teleost epiboly. *Development* **132**, 1105-1116.

Kazmierczak, P., Sakaguchi, H., Tokita, J., Wilson-Kubalek, E. M., Milligan, R. A., Muller, U. and Kachar, B. (2007). Cadherin 23 and protocadherin 15 interact to form tip-link filaments in sensory hair cells. *Nature* **449**, 87-91.

Keller, R. (2002). Shaping the vertebrate body plan by polarized embryonic cell movements. *Science* **298**, 1950-1954.

Keller, R. and Tibbetts, P. (1989). Mediolateral cell intercalation in the dorsal, axial mesoderm of *Xenopus laevis*. *Dev. Biol.* **131**, 539-549.

Kibar, Z., Vogan, K. J., Groulx, N., Justice, M. J., Underhill, D. A. and Gros, P. (2001). Ltap, a mammalian homolog of *Drosophila* Strabismus/Van Gogh, is altered in the mouse neural tube mutant Loop-tail. *Nat. Genet.* **28**, 251-255.

Lefevre, G., Michel, V., Weil, D., Lepelletier, L., Bizard, E., Wolfrum, U., Hardelin, J. P. and Petit, C. (2008). A core cochlear phenotype in USH1 mouse mutants implicates fibrous links of the hair bundle in its cohesion, orientation and differential growth. *Development* **135**, 1427-1437.

Lindqvist, M., Horn, Z., Bryja, V., Schulte, G., Papachristou, P., Ajima, R., Dyberg, C., Arenas, E., Yamaguchi, T. P., Lagercrantz, H. et al. (2010). Vang-like protein 2 and Rac1 interact to regulate adherens junctions. *J. Cell Sci.* **123**, 472-483.

McKenzie, E., Krupin, A. and Kelley, M. W. (2004). Cellular growth and rearrangement during the development of the mammalian organ of Corti. *Dev. Dyn.* **229**, 802-812.

McNeill, H. (2010). Planar cell polarity: keeping hairs straight is not so simple. *Cold Spring Harb. Perspect. Biol.* **2**, a003376.

Mlodzik, M. (2002). Planar cell polarization: do the same mechanisms regulate *Drosophila* tissue polarity and vertebrate gastrulation? *Trends Genet.* **18**, 564-571.

Montcouquiol, M., Rachel, R. A., Lanford, P. J., Copeland, N. G., Jenkins, N. A. and Kelley, M. W. (2003). Identification of Vangl2 and Scrb1 as planar polarity genes in mammals. *Nature* **423**, 173-177.

Muller, U. (2008). Cadherins and mechanotransduction by hair cells. *Curr. Opin. Cell Biol.* **20**, 557-566.

Nagy, I. I., Railo, A., Rapila, R., Hast, T., Sormunen, R., Tavi, P., Rasanen, J. and Vainio, S. J. (2010). Wnt-11 signalling controls ventricular myocardium development by patterning N-cadherin and beta-catenin expression. *Cardiovasc. Res.* **85**, 100-109.

Niessen, C. M., Leckband, D. and Yap, A. S. (2011). Tissue organization by cadherin adhesion molecules: dynamic molecular and cellular mechanisms of morphogenetic regulation. *Physiol. Rev.* **91**, 691-731.

Oteiza, P., Koppen, M., Krieg, M., Pulgar, E., Farias, C., Melo, C., Preibisch, S., Muller, D., Tada, M., Hartel, S. et al. (2010). Planar cell polarity signalling regulates cell adhesion properties in progenitors of the zebrafish laterality organ. *Development* **137**, 3459-3468.

Rauzi, M., Verant, P., Lecuit, T. and Lenne, P. F. (2008). Nature and anisotropy of cortical forces orienting *Drosophila* tissue morphogenesis. *Nat. Cell Biol.* **10**, 1401-1410.

Reynolds, A. B. (2007). p120-catenin: Past and present. *Biochim. Biophys. Acta* **1773**, 2-7.

Roszko, I., Sawada, A. and Solnica-Krezel, L. (2009). Regulation of convergence and extension movements during vertebrate gastrulation by the Wnt/PCP pathway. *Semin. Cell Dev. Biol.* **20**, 986-997.

Ruben, R. J. (1967). Development of the inner ear of the mouse: a radioautographic study of terminal mitoses. *Acta Otolaryngol.* **220 Suppl.**, 1-44.

Senften, M., Schwander, M., Kazmierczak, P., Lillo, C., Shin, J. B., Hasson, T., Geleoc, G. S., Gillespie, P. G., Williams, D., Holt, J. R. et al. (2006). Physical and functional interaction between protocadherin 15 and myosin VIIa in mechanosensory hair cells. *J. Neurosci.* **26**, 2060-2071.

Shimizu, T., Yabe, T., Muraoka, O., Yonemura, S., Aramaki, S., Hatta, K., Bae, Y. K., Nojima, H. and Hibi, M. (2005). E-cadherin is required for gastrulation cell movements in zebrafish. *Mech. Dev.* **122**, 747-763.
Simons, M. and Mlodzik, M. (2008). Planar cell polarity signaling: from fly development to human disease. *Annu. Rev. Genet.* **42**, 517-540.
Steinberg, M. S. (2007). Differential adhesion in morphogenesis: a modern view. *Curr. Opin. Genet. Dev.* **17**, 281-286.
Strutt, H. and Strutt, D. (2009). Asymmetric localisation of planar polarity proteins: Mechanisms and consequences. *Semin. Cell Dev. Biol.* **20**, 957-963.
Tada, M. and Kai, M. (2009). Noncanonical Wnt/PCP signaling during vertebrate gastrulation. *Zebrafish* **6**, 29-40.
Taylor, J., Abramova, N., Charlton, J. and Adler, P. N. (1998). Van Gogh: a new Drosophila tissue polarity gene. *Genetics* **150**, 199-210.
Theisen, H., Purcell, J., Bennett, M., Kansagara, D., Syed, A. and Marsh, J. L. (1994). dishevelled is required during wingless signaling to establish both cell polarity and cell identity. *Development* **120**, 347-360.
Togashi, H., Kominami, K., Waseda, M., Komura, H., Miyoshi, J., Takeichi, M. and Takai, Y. (2011). Nectins establish a checkerboard-like cellular pattern in the auditory epithelium. *Science* **333**, 1144-1147.
Townes, P. L. and Holtfreter, J. (1955). Directed movements and selective adhesion of embryonic amphibian cells. *J. Exp. Zool. A Comp. Exp. Biol.* **128**, 53-120.
Usui, T., Shima, Y., Shimada, Y., Hirano, S., Burgess, R. W., Schwarz, T. L., Takeichi, M. and Uemura, T. (1999). Flamingo, a seven-pass transmembrane cadherin, regulates planar cell polarity under the control of Frizzled. *Cell* **98**, 585-595.
Vinson, C. R. and Adler, P. N. (1987). Directional non-cell autonomy and the transmission of polarity information by the frizzled gene of *Drosophila*. *Nature* **329**, 549-551.
Wallingford, J. B., Rowning, B. A., Vogeli, K. M., Rothbacher, U., Fraser, S. E. and Harland, R. M. (2000). Dishevelled controls cell polarity during Xenopus gastrulation. *Nature* **405**, 81-85.
Wang, J., Mark, S., Zhang, X., Qian, D., Yoo, S. J., Radde-Gallwitz, K., Zhang, Y., Lin, X., Collazo, A., Wynshaw-Boris, A. et al. (2005). Regulation of polarized extension and planar cell polarity in the cochlea by the vertebrate PCP pathway. *Nat. Genet.* **37**, 980-985.
Wang, J., Hamblet, N. S., Mark, S., Dickinson, M. E., Brinkman, B. C., Segil, N., Fraser, S. E., Chen, P., Wallingford, J. B. and Wynshaw-Boris, A. (2006a). Dishevelled genes mediate a conserved mammalian PCP pathway to regulate convergent extension during neurulation. *Development* **133**, 1767-1778.
Wang, Y., Guo, N. and Nathans, J. (2006b). The role of Frizzled3 and Frizzled6 in neural tube closure and in the planar polarity of inner-ear sensory hair cells. *J. Neurosci.* **26**, 2147-2156.
Wilson, P. and Keller, R. (1991). Cell rearrangement during gastrulation of *Xenopus*: direct observation of cultured explants. *Development* **112**, 289-300.
Xiao, K., Oas, R. G., Chiasson, C. M. and Kowalczyk, A. P. (2007). Role of p120-catenin in cadherin trafficking. *Biochim. Biophys. Acta* **1773**, 8-16.
Yamamoto, N., Okano, T., Ma, X., Adelstein, R. S. and Kelley, M. W. (2009). Myosin II regulates extension, growth and patterning in the mammalian cochlear duct. *Development* **136**, 1977-1986.
Zallen, J. A. and Wieschaus, E. (2004). Patterned gene expression directs bipolar planar polarity in *Drosophila*. *Dev. Cell* **6**, 343-355.
Zallen, J. A. and Blankenship, J. T. (2008). Multicellular dynamics during epithelial elongation. *Semin. Cell Dev. Biol.* **19**, 263-270.